# Convergent evolutionary reduction of atrial septation in lungless salamanders

Journal of Anatomy

*J. Anat.* (2016) doi: 10.1111/joa.12535

# Convergent evolutionary reduction of atrial septation in lungless salamanders

Zachary R. Lewis and James Hanken

*Department of Organismic and Evolutionary Biology, and Museum of Comparative Zoology, Harvard University, Cambridge, MA, USA*

## Abstract

Nearly two thirds of the approximately 700 species of living salamanders are lungless. These species respire entirely through the skin and buccopharyngeal mucosa. Lung loss dramatically impacts the configuration of the circulatory system but the effects of evolutionary lung loss on cardiac morphology have long been controversial. For example, there is presumably little need for an atrial septum in lungless salamanders due to the absence of pulmonary veins and the presence of a single source of mixed blood flowing into the heart, but whether lungless salamanders possess an atrial septum and whether the sinoatrial aperture is located in the left or right atrium are unresolved; authors have stated opposing claims since the late 1800s. Here, we use micro-computed tomography (μ-CT) imaging, gross dissection and histological reconstruction to compare cardiac morphology among lungless plethodontid salamanders (Plethodontidae), salamanders with lungs, and the convergently lungless species *Onychodactylus japonicus* (Hynobiidae). Plethodontid salamanders have partial atrial septa and incomplete separation of the atrium into left and right halves. Partial septation is also seen in *O. japonicus*. Hence, lungless salamanders from two lineages convergently evolved similar morphology of the atrial septum. The partial septum in lungless salamanders can make it appear that the sinoatrial aperture is in the left atrium, but this interpretation is incorrect. Outgroup comparisons demonstrate that the aperture is located in a posterodorsal extension of the right atrium into the left side of the heart. Independent evolutionary losses of the atrial septum may have a similar developmental basis. In mammals, the lungs induce formation of the atrial septum by secreting morphogens to neighboring mesenchyme. We hypothesize that the lungs induce atrial septum development in amphibians in a similar fashion to mammals, and that atrial septum reduction in lungless salamanders is a direct result of lunglessness.

**Key words:** atrial septum; axolotl; evo-devo; homoplasy; lung; lunglessness; Plethodontidae; salamander.

## Introduction

Integrated organ systems are hallmarks of bilaterian life. However, such integration may also constrain potentially adaptive evolutionary changes (Gould, 1980). Saltatory changes to single organs, such as organ loss, may be maladaptive within interconnected organ systems because of the need for the system as a whole to function in order to maintain organismal fitness. These constraints can be circumvented by pleiotropy, whereby single genes govern development of multiple organs, or by evolved molecular interactions between organ systems that ensure matching morphologies develop in tandem. An example of the latter may be found in the cardiopulmonary system. In terrestrial vertebrates, the heart and lungs function as an integrated system. Complete cardiac septation, including the development of ventricular and atrial septa, has evolved convergently twice, each time providing separation of oxygenated and deoxygenated blood and efficient gas exchange (Koshiba-Takeuchi *et al.* 2009; Jensen *et al.* 2013). Molecular signals secreted from the developing lungs mediate the development of the atrial septum. Indeed, the lungs may provide cues to the heart that enable the functional integration of both organs (Hoffmann *et al.* 2009, 2014). This interaction provides one paradigm for understanding how the lungs and heart are capable of correlated development, and thus correlated evolution.

Complete cardiac septation, resulting in a four-chambered heart, is found only within mammals and archosaurs. Amphibians typically have a three-chambered heart, with a septate atrium and an undivided ventricle (Noble, 1925).

*Correspondence*
*Zachary R. Lewis, Department of Ecology and Evolutionary Biology, Brown University, Providence, RI 02912, USA. E: zrlewis@gmail.com*

Accepted for publication *14 July 2016*

Yet, and despite the lack of ventricular septation, deoxygenated and oxygenated blood streams mostly remain separate as they pass through the heart (Noble, 1925; de Graaf, 1957; Johansen, 1962; Haberich, 1965). Separation of pulmonary and systemic blood streams may be achieved due to the action of the spiral septum within the conus arteriosus (Noble, 1925).

Atrial septum development is best understood in mammals, in part due to the high prevalence of human atrial septal defects (ASDs). Congenital ASDs are among the most common birth defects (Parker *et al.* 2010; Bjornard *et al.* 2013). This has prompted several recent investigations into both the development of the atrial septum (AS) in mammals (Goddeeris *et al.* 2008; Hoffmann *et al.* 2009, 2014; Xie *et al.* 2012) and the genetic basis of certain AS malformations, such as those associated with Holt-Oram Syndrome (Basson *et al.* 1997), which is caused by mutations in the T-box protein Tbx5 (Li *et al.* 1997). The mammalian atrial septum develops from multiple tissues, including the primary atrial septum with a mesenchymal cap, the second heart field-derived dorsal mesenchymal protrusion (DMP), and the atrioventricular cushions (Jensen & Moorman, 2016; Wessels, 2016). The DMP portion of the AS develops in close association with the pulmonary vein (Briggs et al. 2012) and deficiency of this tissue results in atrioventricular septal defects (Goddeeris *et al.* 2008; Hoffmann *et al.* 2009, 2014).

Although atrial septum development is well characterized in mammals, much of the morphological and developmental diversity of atrial septa across tetrapods awaits description (Mohun *et al.* 2000; Jensen *et al.* 2013; de Bakker *et al.* 2015). As in mammals, the amphibian atrial septum emerges from the dorsal wall of the atrium and grows posteroventrally towards the atrioventricular aperture (Mohun *et al.* 2000). The atrial septum of adult salamanders is composed of two main components. The first component is a sheet of tissue, oriented approximately 45° oblique to the sagittal plane, that stretches from the dorsal border of the atrium near the sinoatrial aperture to the atrioventricular aperture. The sinoatrial valve is attached to its right dorsal portion. The second component is a sheet of tissue connected to the left side of the first component that stretches to the left wall of the atrium (Putnam & Parkerson, 1985). Together, these two components functionally subdivide the atrium into left and right halves (Davies & Francis, 1941). Fenestration of the first component is frequently described in salamanders, particularly those species with less reliance on pulmonary respiration (Noble, 1925 and references therein).

Although amphibians descended from ancestors with lungs, lungless species or clades have originated at least four times independently across all living orders (Wilder, 1896; Noble, 1925; Nussbaum & Wilkinson, 1995; Bickford *et al.* 2008). Lung loss is a remarkable example of morphological convergence, or homoplasy, yet little attention has been paid to the corresponding morphology of the circulatory system in lungless species. Moreover, all previous work has focused on only a single lineage of lungless salamanders, the family Plethodontidae. Adult plethodontids are completely lungless salamanders that respire cutaneously and through the buccopharyngeal mucosa (Whitford & Hutchison, 1965). Despite several studies of this one group, the degree of atrial septation in plethodontid salamanders has long been controversial. Gross dissection of plethodontid hearts has yielded a number of contradictory hypotheses regarding atrial septum morphology (Fig. 1).

The morphology of the plethodontid AS, and even its presence or absence, has been contentious since the end of the 19th century. The atrial septum is thin and delicate, which may contribute to the difficulty in resolving contradictory hypotheses. In addition, each previous study used different fixation techniques and examined a different plethodontid species, sometimes without comparison with a lunged outgroup (Hopkins, 1896; Bruner, 1900; Noble, 1925; Putnam & Kelly, 1978). No attempt has been made to study this structure using even standard histology, let alone more advanced visualization methods such as three-dimensional reconstruction from computed tomography (CT) or histological datasets. Approaches that incorporate novel morphological techniques and broad comparative datasets may help to reconcile the conflicting hypotheses on the plethodontid AS and yield greater understanding of the evolution of integrated organ systems in general.

Among the few non-plethodontid lungless amphibians is the hynobiid salamander genus *Onychodactylus* from mainland Asia and Japan (Yoshikawa *et al.* 2008; Yoshikawa & Matsui, 2014). Heart morphology in *Onychodactylus* has not been examined, despite its relevance to the unresolved hypotheses regarding of the morphology of the heart of other lungless amphibians. Exploring the mechanisms and consequences of lung loss in *Onychodactylus* will enable a better understanding of the basis of convergent evolution among lungless clades.

Here we employ several techniques to examine AS morphology across six families of lungless and lunged salamander species (Table 1). Histological sectioning and three-dimensional reconstruction are combined with gross dissection and contrast-stained micro-CT (μ-CT) to describe atrial septum morphology and variation in detail. Unlike lunged salamanders, which have a two-part AS, plethodontids possess a partial AS due to conservation of the first atrial septum component but not the second. The partial septum of plethodontids would be unable to maintain separation of blood from left and right atria. Atrial morphology of the convergently lungless salamander *Onychodactylus japonicus* is similar to that of plethodontids and evolved independently.

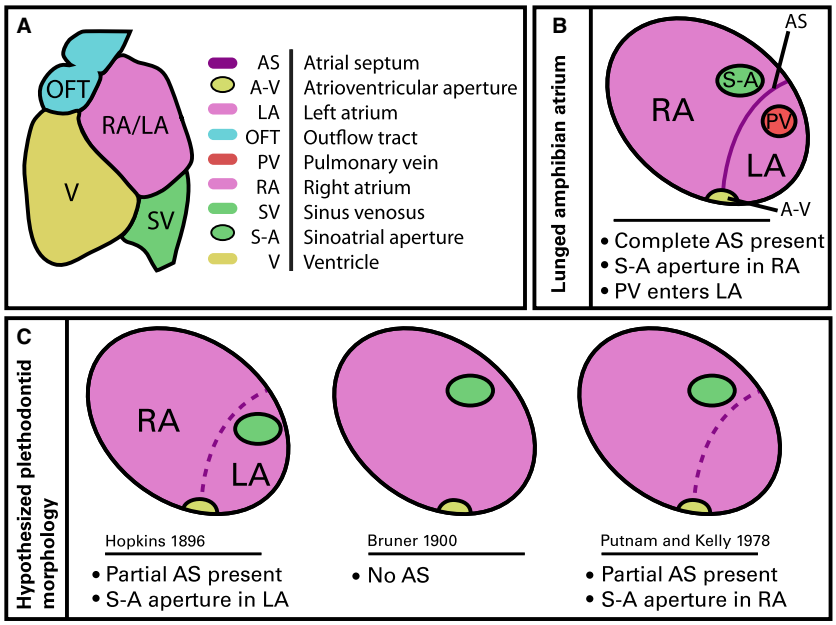


**Fig. 1.** Previous hypotheses on the morphology of the plethodontid atrium. (A) Abbreviations, color schema and general heart morphology from a ventral perspective. Anterior is at the top. (B) Generalized morphology of the atrium of an amphibian with lungs. Schematic of a transverse section. (C) Three hypotheses on the morphology of the atrium in plethodontid (lungless) salamanders. The hypotheses differ regarding the location of the sinoatrial aperture and whether an atrial septum is present.

**Table 1** List of specimens and stages examined.

| Species | Stage (Sample size) | Specimen No. | Techniques* |
|---|---|---|---|
| Lunged species | | | |
| *Ambystoma mexicanum* | 44 (1), 52 (1), 57 (2), adult (1) | N/A | H, μ, D |
| *Amphiuma tridactylum* | Adult (1) | MCZ A-115797 | D |
| *Andrias japonicus* | Juvenile (1) | MCZ A-119843 | μ |
| *Cynops ensicauda* | Adult (1) | MCZ A-26607 | D |
| *Hynobius nigrescens* | Adult (1) | MCZ A-22511 | μ |
| Lungless species | | | |
| *Desmognathus fuscus* | Larvae (2) | N/A† | H |
| *Desmognathus quadramaculatus* | Adult (1) | MCZ A-117899 | D |
| *Hemidactylium scutatum* | Embryo (1), late larva (4), adult (1) | N/A† | H, μ |
| *Plethodon glutinosus* | Adult (1) | MCZ Z-27269 | D |
| *Plethodon cinereus* | Embryo (2), hatchling (1), adult (4) | N/A† | H, μ |
| *Pseudotriton montanus* | Adult (1) | MCZ A-5739 | D |
| *Onychodactylus japonicus* | Late larva (1) | MCZ A-119652 | μ |

*D, dissection; H, histology; μ, X-ray μ-CT.
†Locality provided in Supporting Information Table S1.

## Material and methods

### Animal collection and husbandry

*Ambystoma mexicanum* (axolotl) embryos were procured from the Ambystoma Genetic Stock Center, University of Kentucky, and maintained in 20% Holtfreter solution (12 mM NaCl, 0.12 mM KCl, 0.18 mM $CaCl_2$, 0.04 mM $NaHCO_3$) at 17 °C. All plethodontid embryos were collected under Massachusetts Department of Fish and Wildlife permits and local permits, where applicable. DFW permit numbers: 181.10SCRA (2010), 080.11SCRA (2011), 080.11SCRA (2012), 027.13SCRA (2013), 083.14SCRA (2014), and 022.15SCRA (2015). Locality data are provided in Supporting Information Table S1. *Hemidactylium scutatum* embryos were collected at Cape Cod National Seashore (permit CACO-2012-SCI-0008) and maintained in the lab on filter paper moistened with 0.1x MMR (Marc's Modified Ringer solution: 0.01 M NaCl, 0.2 mM KCl, 0.1 mM $MgSO_4$, 0.2 mM $CaCl_2$, 0.5 mM HEPES pH 7.4) with 100 μg $mL^{-1}$ gentamicin (Sigma, St. Louis, MO, USA) at 15 °C. At hatching, they were transferred to 20% Holtfreter solution and fed *Artemia* spp. until fixation with Bouin fixative. *Plethodon cinereus* embryos were typically collected from underneath moss atop fallen hemlock logs or inside rotting hemlock logs. They were maintained in the lab at 15–17 °C on filter paper moistened with 0.1x MMR and 100 μg $mL^{-1}$ gentamicin or fully immersed in the same solution. Better success was obtained by raising embryos in solution. *Plethodon cinereus* embryos were monitored daily for fungal infections and to assess developmental stage, until fixation before or at hatching in 10% neutral-buffered formalin (NBF) or Bouin fixative.

*Desmognathus fuscus* embryos were field-collected and raised similarly to *P. cinereus* embryos until hatching, then maintained as larvae in 20% Holtfreter solution and fed *Artemia* spp. until fixation.

*Ambystoma mexicanum* were staged according to Bordzilovskaya *et al.* (1989) and Nye *et al.* (2003). *Hemidactylium scutatum* animals were staged according to Hurney *et al.* (2015). *Plethodon cinereus* embryos were staged according to Kerney (2011).

### Museum specimens and gross dissection

Specimens examined are listed in Table 1. Dissections were carefully performed with a scalpel, fine scissors and #5 forceps in order to not tear the delicate atrial septum. Congealed blood was removed from the atria manually and by rinsing with 70% ethanol.

### Micro-computed tomography

For X-ray μ-CT, freshly sacrificed specimens were fixed in 10% NBF, washed with 1× phosphate-buffered saline and then dehydrated in 70% ethanol. Specimens (with the exception of *Andrias japonicus* and *Hynobius nigrescens*) were soaked in 2.5% phosphomolybdic acid (Sigma) in 70% ethanol for 1–2 weeks, washed briefly with 70% ethanol, and embedded in 0.8% agarose to stabilize the specimen and prevent desiccation (Metscher, 2011). 360-degree μ-CT scans at 0.1-degree increments were run at 80 kV, 70 μA, and 800 ms exposure time at pixel dimensions of 5.3–9.9 μm, on a SkyScan 1173 benchtop scanner (Bruker μ-CT, Kontich, Belgium). *Andrias japonicus* and *H. nigrescens* were stained with 1% $I_2$ in 70% ethanol for 7 days, then scanned with 360-degree μ-CT scans at 0.2-degree increments at 80 kV, 100 μA, and 1000 ms exposure time at pixel dimensions of 24 μm (*A. japonicus*) and 11 μm (*H. nigrescens*) on a SkyScan 1173 benchtop scanner. Reconstruction was performed with the native reconstruction software using ring-artifact reduction and post-alignment corrections where appropriate (NRecon, Bruker μ-CT, Kontich, Belgium). Reconstructed TIFF files were visualized in AMIRA 6.0 (FEI, Hillsboro, OR, USA) and segmented using the segmentation editor. Separate label fields were utilized for the septal and endocast components so their opacity could be adjusted independently. CT data are available for download at: https://dataverse.harvard.edu/dataverse/atrialseptation.

### Histology and histological reconstruction

Specimens were fixed in Bouin solution for 24–48 h prior to washing, dehydrating and embedding in paraplast (McCormick Scientific, Wetzlar, Germany). Serial sections (7 or 8 μm) were stained using the Mallory trichrome method (Presnell *et al.* 1997) with the following modifications: a 10-min stain in Mayer hematoxylin followed by a 10-min wash in running reverse-osmosis (RO) $H_2O$ preceded 30 s in 1% acid fuchsin, several rinses with RO $H_2O$, 5 min in 1% phosphomolybdic acid, then 3 min in a modified Mallory II (1% orange G, 1% aniline blue, and 2% oxalic acid) followed by dehydration and mounting. In salamanders, this staining procedure typically resolves collagen and connective tissue as bright blue, muscle and epithelia as purple and blood as bright red. Sections were imaged using a Leica DMRE microscope (Wetzlar, Germany) equipped with a QImaging Retiga 2000r camera and a QImaging RGB slider (Surrey, Canada) and VOLOCITY 6.0 software (PerkinElmer, Waltham, MA, USA). Monochrome images were imported into AMIRA and aligned using the Align Slices module. Endocasts of cardiac chambers were made using segmentation tools in AMIRA, as described above. Reconstruction was performed only on specimens with nearly complete or complete serial sections. In the event that a section was damaged or distorted, labels were interpolated from the flanking slides.

## Results

### Lunged salamanders develop a two-part atrial septum

In terms of gross morphology, the salamander heart is composed of a sinus venosus (SV), atrium, ventricle and outflow tract (OFT) (Fig. 2A). The SV is supplied by the left and right common cardinal veins and the posterior cardinal vein. It is situated dorsal to the atria, and the two chambers overlap at their anterior and posterior halves, respectively. The sinoatrial aperture (S-A) leads from the SV into the right atrium. The left and right atria are not distinguishable externally, but they are separated internally by the atrial septum, described below. Pulmonary venous blood from the lungs enters the heart through the left and right pulmonary veins, which fuse dorsal to the SV to become the common pulmonary vein and supply the left atrium. The ventricle is situated ventral to and to the right of the atria. Blood from the atria flows through the atrioventricular aperture (A-V) into the ventricle. The atrioventricular valve is composed of two wide semilunar leaflets oriented in the frontal plane, one dorsal and the other ventral (Fig. 2E). The ventricle, while undivided, is traversed by a network of trabeculae. The OFT is separated from the ventricle by a set of three semilunar valves. The outflow tract is composed of the proximal conus arteriosus and distal truncus arteriosus, which are separated by a set of valves. The spiral septum lies within the conus arteriosus.

In all lunged salamanders we examined, the atrial septum comprises two perpendicularly oriented, interconnected endocardial-type tissues, AS1 and AS2 (Fig. 2). These tissues appear to correspond to components 'IA' and 'IB,' respectively, described by Putnam & Kelly (1978). AS1 is a thin sheet oriented approximately 45° from the sagittal plane. From its caudal edge at the center of the A-V, it stretches approximately 45° leftward to the cranial wall of the atrium. AS1 is emarginated posterodorsally, forming an arch under which blood flows from the S-A into the right atrium (RA; Fig. 2E,F). AS2 is oriented dorsoventrally; it attaches to the left side of AS1 and stretches to the left wall of the atrium (Fig. 2E). Removal of the ventral atrial wall reveals AS2, and further excision of AS2 reveals the S-A posterodorsal to it (Supporting Information Fig. S3). The pulmonary vein (PV) lies on the SV dorsally and enters the left atrium (LA) at its anterodorsal surface, anteroventral to AS2 (Fig. 2B). An orifice in AS2 near the A-V allows blood to pass from the LA to the ventricle. This orifice is small in adult *Cynops ensicauda* but much larger in juvenile

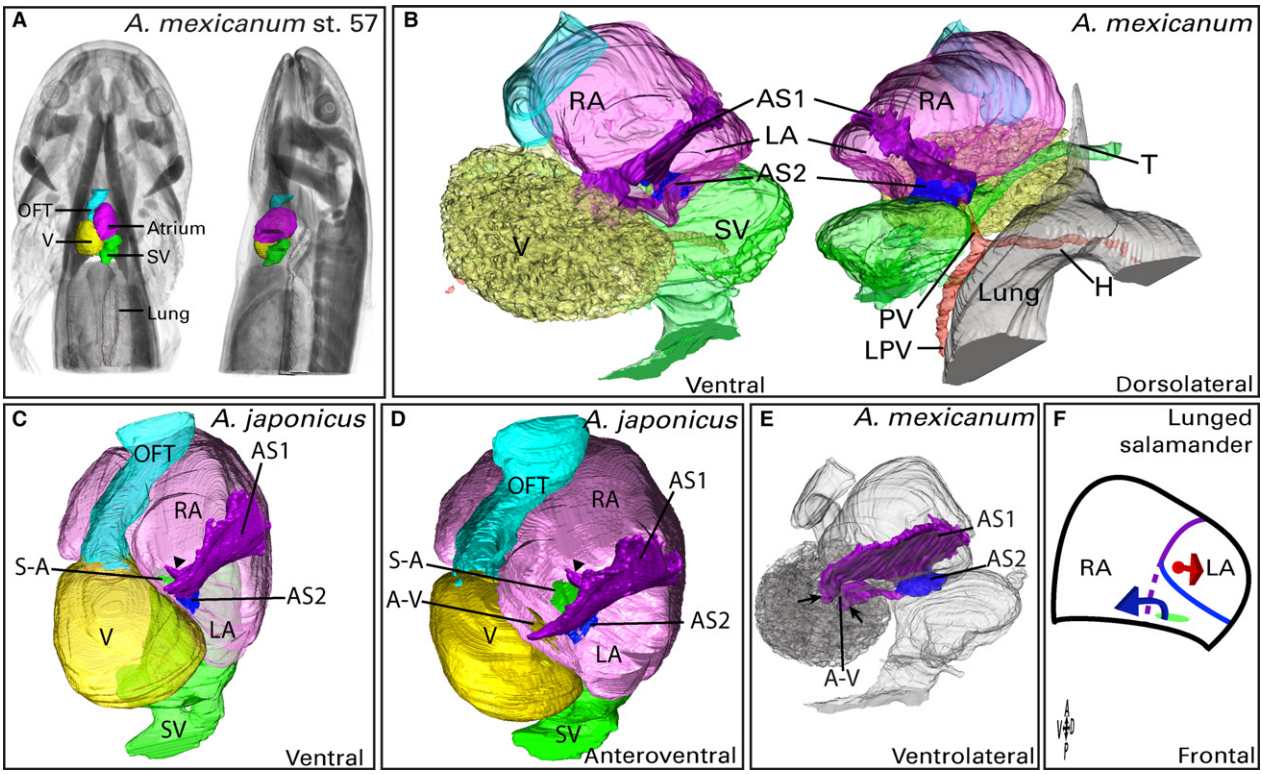


**Fig. 2.** Atrial morphology in lunged salamanders. (A) Contrast μ-CT of a stage-57 (juvenile) axolotl, *Ambystoma mexicanum*, depicted in ventral (left) and lateral perspectives. (B) Reconstruction of the *A. mexicanum* heart at stage 57 generated from 8-μm histological sections. The ventral portion of the trachea (T), hilus (H) and lungs are visible in the dorsolateral view. (C, D) The heart of the Japanese giant salamander, *Andrias japonicus* (26.5 cm total length, 16.5 cm snout-vent length) in ventral (C) and anteroventral (D) views. The sinoatrial valve is visible as a rightward projection from the posterodorsal portion of AS1 (arrowheads). (E) Components of the atrial septum are highlighted in a stage-57 *A. mexicanum* heart, shown from a ventrolateral perspective. The chambers of the heart have been rendered in grayscale. Both leaflets of the atrioventricular valve are rendered in purple, as they are continuous with the atrial septal complex (arrows). (F) Schematic frontal section of a lunged salamander atrium, showing the location of the pulmonary vein (red), S-A (green) and associated blood streams. AS1, atrial septum component 1; AS2, atrial septum component 2; A-V, atrioventricular aperture; LA, left atrium; LPV, left pulmonary vein; OFT, outflow tract; PV, common pulmonary vein; RA, right atrium; S-A, sinoatrial aperture; SV, sinus venosus; V, ventricle.

*A. mexicanum* (Figs 2E and S3). In histological sections of the atrial septum at juvenile stages, both AS1 and AS2 are endocardial-type tissues distinguished only by their orientation (Supporting Information Figs S1 and S2).

The AS1 in *A. mexicanum* takes several weeks to fully form. Its rostral portion is completely developed at early post-embryonic stages, yet at post-embryonic stage 52 (2–3 weeks post-hatching) there remains a gap caudally, resulting in the confluence of the RA and LA (Fig. S1). The separation of left and right atria is nearly complete by stage 57 (subadult) (Fig. S2), but there remains a small gap between AS1 and the caudal wall of the atrium (Fig. 2, Supporting Information Figs S1 and S2, Videos S1 and S2). Adult *A. mexicanum* have a complete AS1 as determined by gross dissection (not shown); blood from the PV passes ventral to AS2. Prior to complete development of AS1, pulmonary venous blood from the PV could potentially mix with deoxygenated blood from the RA before passing through the A-V. However, when viewed anteriorly, the AS2 completely covers the S-A and thus would likely direct blood from the SV into the RA and maintain oxygenated blood from the PV in the LA (Fig. 2). Adult *A. mexicanum* possess a well-developed AS1, thus facilitating separation of the two blood streams.

To evaluate the condition of the atrial septum in a closely related outgroup to plethodontid salamanders, we dissected a specimen of *Amphiuma tridactylum* (Amphiumidae). Molecular phylogenies consistently place the family Amphiumidae as the sister group to Plethodontidae (Pyron & Wiens, 2011). Our dissection agrees with previously published findings (Johansen, 1963). *Amphiuma tridactylum* has a large LA separated from the RA by a robust, imperforate atrial septum (data not shown). To determine the likely ancestral state of atrial septation in salamanders we generated and analyzed contrast-enhanced μ-CT data from two phylogenetically basal salamander species, *Andrias japonicus* (Cryptobranchidae; Fig. 2C,D) and *Hynobius nigrescens* (Hynobiidae; data not shown). Both species have a well-developed atrial septum complex that separates the left and right atria. The

sinoatrial valve is clearly visible in *A. japonicus* as a flap at the posterodorsal base of AS1 (Fig. 2C,D).

We found no indication of fenestration or perforation of the atrial septum in *A. mexicanum*. While we observed no gross signs of atrial septum fenestration in *C. ensicauda* or *A. tridactylum*, our reliance on gross dissection alone in these species makes us unable to rule out fenestration. A spiral valve is present in the conus arteriosus of *A. mexicanum*.

### Lungless plethodontid salamanders lack AS2

Several species of plethodontid salamanders were dissected, sectioned histologically, or subjected to contrast-stained μ-CT imaging (Table 1). The atrial chamber of plethodontids broadly resembles that of salamanders with lungs: AS1 is present and oriented at a 45-degree angle to the sagittal plane, it lacks perforations, and its dorsal border is emarginate (Figs 3 and 4). Thus, AS1 in these lungless salamanders is morphologically similar to AS1 in lunged salamanders in that it occupies the same position in the heart and is not fenestrated.

Plethodontids, however, lack AS2, resulting in incomplete atrial septation (Fig. 3B,C,E; Supporting Information Video S3). Since AS2 essentially forms the dorsal wall of the LA in lunged salamanders, its absence results in complete confluence of left and right atria. Plethodontids also lack pulmonary veins; all inflow to the heart is through the left and right common cardinal veins (ducts of Cuvier) and the posterior cardinal vein, which empty into the SV. Blood enters the atrium solely through the S-A from which it would presumably flow to either side of AS1 before passing through the A-V during atrial systole. Consistent with published studies (Noble, 1925), we did not observe a spiral valve in plethodontids (Fig. 4).

Previous authors disagree on the position of the S-A in plethodontids (Fig. 1). Our gross dissection reveals that the S-A is to the left of AS1 when the atrium is viewed ventrally (Fig. 3C). However, the LA in lunged salamanders is bordered by the AS1 medially and the AS2 dorsally (Figs 2 and

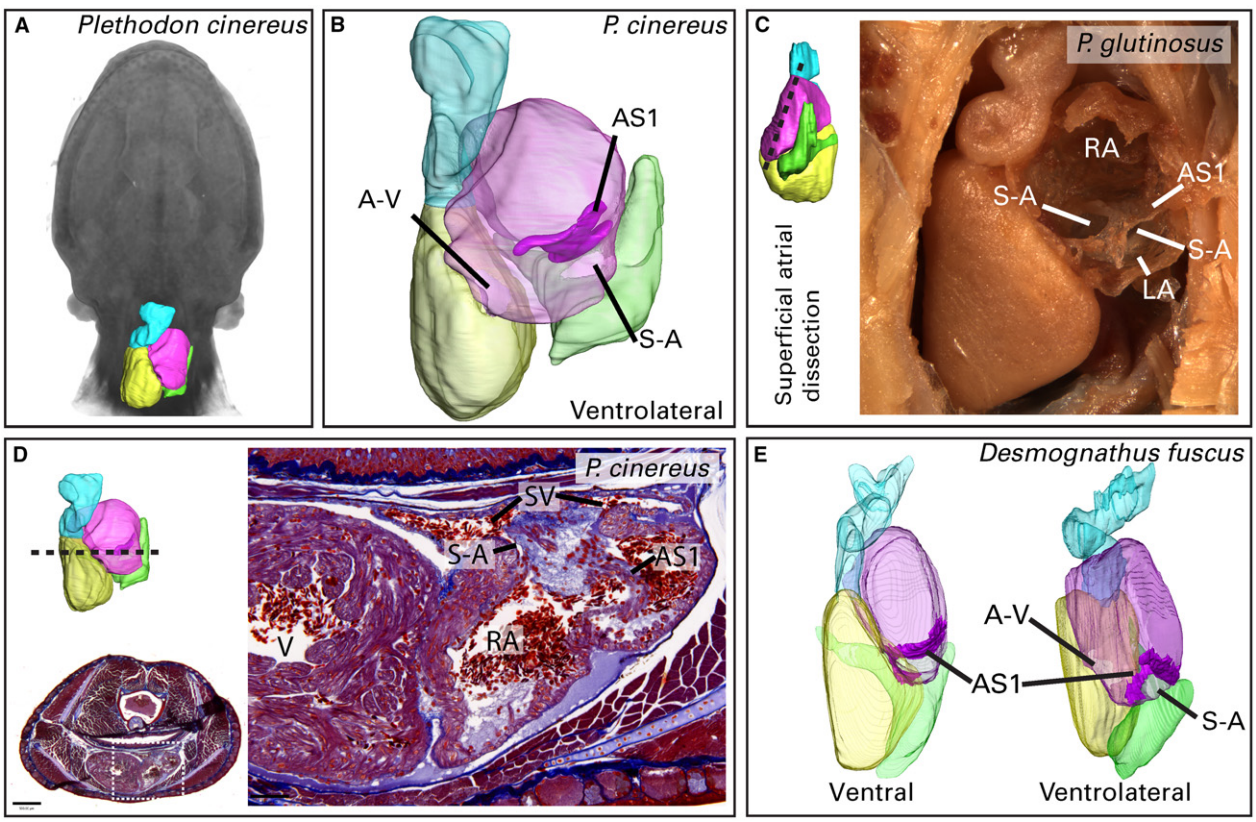


**Fig. 3.** Atrial morphology in plethodontid salamanders. (A) Contrast μ-CT of a *Plethodon cinereus* embryo at hatching (stage 24; Kerney, 2011). Heart chambers have been segmented and colored. (B) Stage-24 *P. cinereus* heart magnified to show the atrial septum. Only AS1 is present. Ventrolateral perspective. (C) Atrium of an adult *Plethodon glutinosus*. The plane and angle of dissection are indicated by the colored reconstruction. Ventral view. (D) Transverse section through the atrial septum of an adult *P. cinereus*. The approximate plane is indicated in the schematic on the upper left. Boxed area at lower left is enlarged in image on the right. Scale bars 500 μm and 100 μm for left and right images, respectively. (E) Reconstruction of the heart of a *Desmognathus fuscus* larva (25 mm total length, 14.5 mm snout-vent length) in ventral and left ventrolateral views. AS1, atrial septum component 1; A-V, atrioventricular aperture; LA, left atrium; OFT, outflow tract; RA, right atrium; S-A, sinoatrial aperture; SV, sinus venosus.

7). Absence of AS2 thus can give the impression that the S-A lies within the left atrium, but a comparative approach demonstrates that this impression is incorrect (Figs 4, 5 and 7).

The dorsal base of AS1 in adult *P. cinereus* is composed of endocardial and myocardial tissue (Supporting Information Fig. S4). The portion of AS1 that traverses the atrial chamber from its dorsal attachment to the A-V is myocardial in adults. However, AS1 is a wholly endocardial-type tissue in embryos, similar to juvenile *A. mexicanum*. In adult *P. cinereus*, the portion of the endocardial base flanking the S-A protrudes into the right atrium as a flap and likely functions as a sinoatrial valve (Figs 3D and S4B,C).

Either of two ontogenetic scenarios could account for the cardiac morphology of adult plethodontids. First, the atrial septum may develop fully and subsequently regress. Alternatively, the atrial septum may never develop fully. Our data support the latter scenario. By reconstructing hearts from plethodontids at stages ranging from hatchling to late larva to adult, we find no sign of AS2 at any point in development in any species (Fig. 3).

### Lungless *Onychodactylus japonicus* also lacks AS2

The heart from a single larval specimen of *Onychodactylus japonicus* (Hynobiidae) (6.5 cm total length, 3.5 cm snout–vent length) was examined by using contrast μ-CT (Fig. 6). AS1 is clearly visible as a region within the atria devoid of blood (Fig. 6). In contrast to plethodontids, where a dorsal emargination of AS1 would cause blood to first flow dorsally and then posteriorly towards the A-V, AS1 is emarginated posteroventrally in *O. japonicus* . Blood likely flows from the S-A posteroventrally around the free margin of AS1 and then through the A-V. There is no AS2, and the left atrium is extremely small.

## Discussion

By examining cardiac morphology in a diverse sample of plethodontid salamanders, lunged salamanders, and the convergently lungless species *Onychodactylus japonicus*, we demonstrate that two lineages of lungless salamanders independently evolved similar atrial morphology, including the loss of a significant component of the atrial septum (AS). Our work is the first description of the atrial morphology of *O. japonicus*. Previous studies of plethodontid heart morphology left several questions unresolved. In particular, the position of the sinoatrial aperture (S-A) and the presence or absence of the atrial septum have been debated for over 100 years (Fig. 1). Recent advances in computer-assisted, 3-dimensional reconstruction from histological or tomographic datasets facilitates study of the complex hearts of salamanders.

Given the presence of AS1 and AS2 in cryptobranchid, amphiumid, ambystomatid and salamandrid salamanders (present study; Davies & Francis, 1941; Johansen, 1963; Putnam & Parkerson, 1985), combined with published data on septation in frogs and caecilians (Noble, 1925; de Bakker *et al.* 2015), we infer the basal condition for salamanders to be fully septate. Hence, the morphology of lungless salamanders represents an evolutionary loss of a prominent portion of the atrial septum, AS2 (Fig. 7C).

### Why lose the septum?

Although some species of plethodontids retain the pulmonary arch, adult lungless amphibians lack pulmonary veins (McMullen, 1938). Consequently, all blood flowing into the heart originates from the left and right common cardinal veins (ducts of Cuvier) and the posterior cardinal vein via the sinus venosus (Barrows, 1900; Seelye, 1906; McMullen, 1938). Since this blood is from a single mixed source, lungless amphibians do not require separation of blood in the heart. In fact, the presence of an AS might be disadvantageous in this situation, which could lead to extreme pressure differentials between atrial chambers.

In humans, anomalies of pulmonary venous return are developmental defects which entail anastomosis of the pulmonary veins to the right inflow tract. These misconnections may cause extreme pressure differentials between RA and LA (Taussig, 1960; El-Said *et al.* 1972); patients may die due to the high load on the right side of the heart. Survival is possible if a patient possesses compensatory defects in the AS that relieve the pressure differential or if the patient undergoes surgical intervention (El-Said *et al.* 1972). The physiological disadvantage of left–right pressure differential resulting from the lack of pulmonary veins might have selected for atrial septum reduction during the evolution of lunglessness in salamanders. If so, then lungless salamanders have evolved a condition similar to a human atrial septal defect in response to the unique configuration of their cardiac inflow. Salamanders may offer a beneficial model for the study of atrial septal defects or anomalous pulmonary venous return.

Our hypothesis that fully developed atrial septation is maladaptive when pulmonary return is reduced or absent due to the resulting blood pressure differential between atrial chambers contrasts with the the generally accepted hypothesis regarding the reduction of atrial septation in lungless or lung-reduced salamanders. Johansen and Hanson (1968) proposed that atrial septum reduction is due to relaxed selective pressure to retain atrial septation because cutaneous respiration results in systemic blood high in oxygen. Our alternative hypothesis is based on the strong correlation between lung loss/reduction and atrial septum reduction as well as the demonstrated deficits associated with anomalous pulmonary venous return in humans.

Atrial septum reduction is unlikely to be a passive consequence of the loss of pulmonary return. The AS develops normally over 90% of the time in tadpoles in which

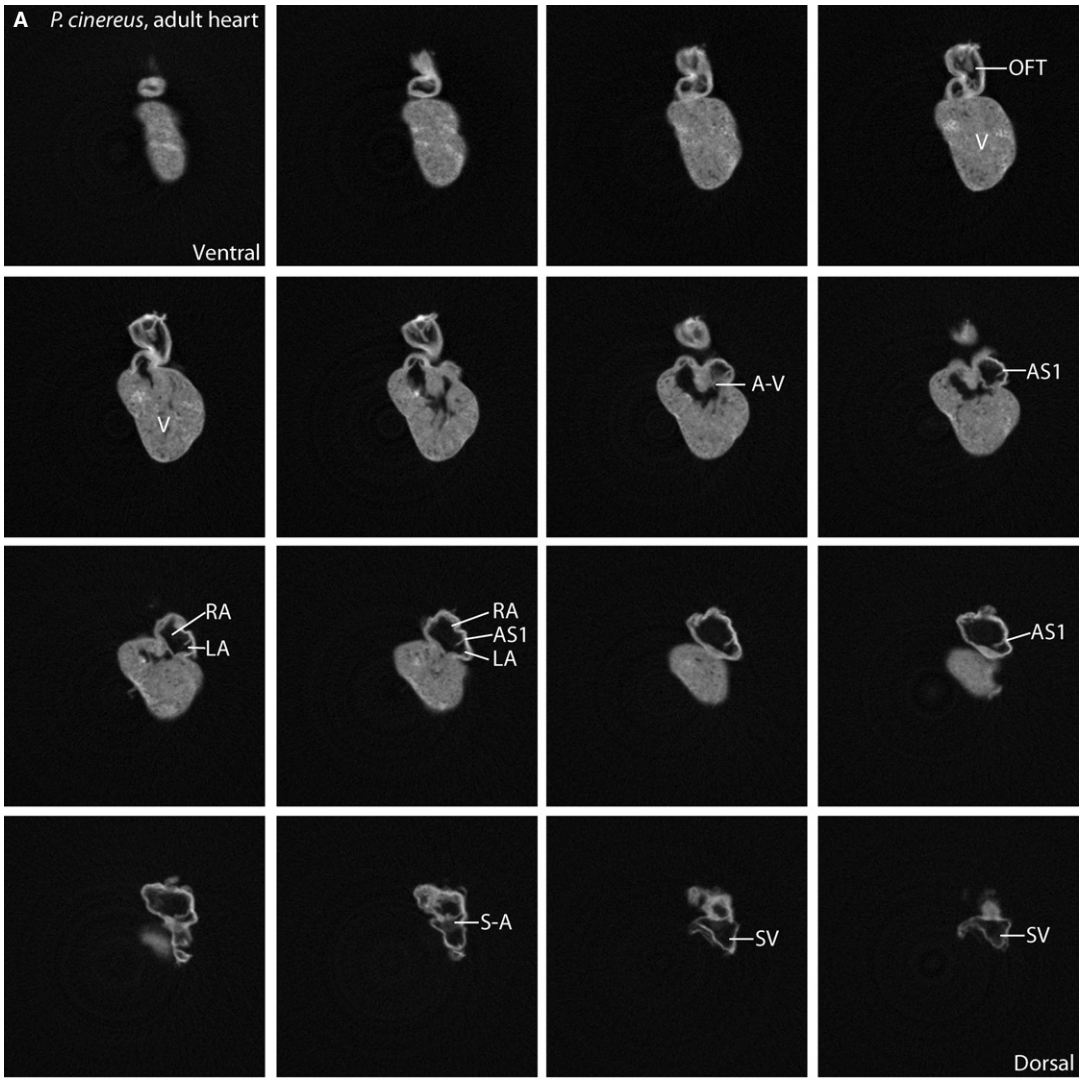


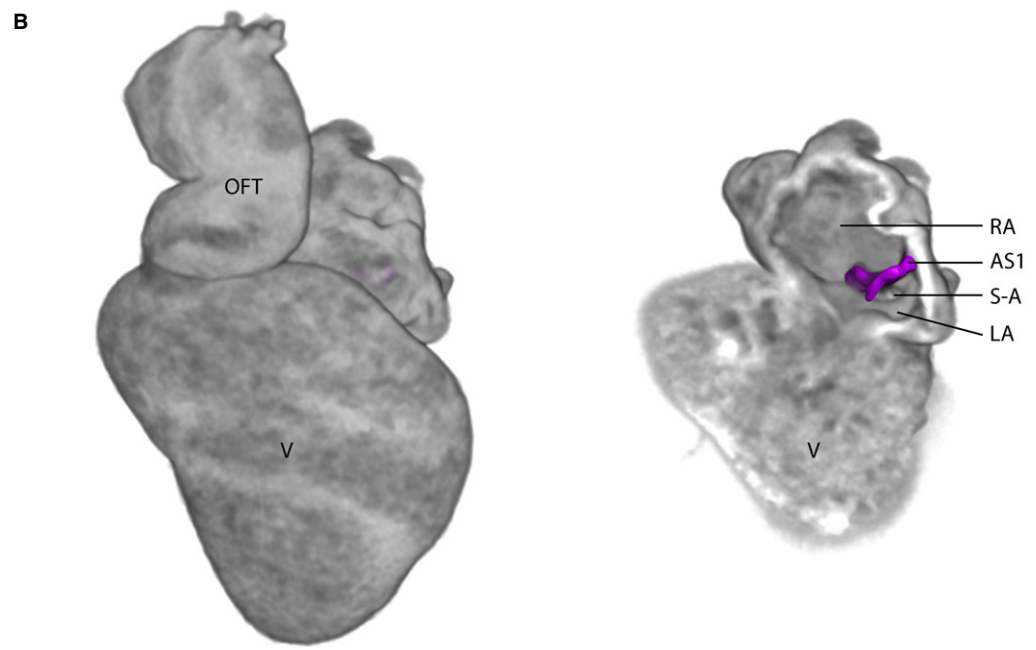

pulmonary return was ablated by lung extirpation just prior to the development of the AS (Simons, 1957). The abnormal AS morphologies observed at low frequency can be attributed to mechanical damage during surgery (Simons, 1957).

### Atrial septum controversy

Atrial morphology in plethodontids has been contentious, with no agreement regarding even basic features such as the presence or absence of a septum, the position of the S-A and the degree of septal fenestration (Noble, 1925; Putnam & Kelly, 1978; Fig. 1). In the first published work on plethodontid hearts, Hopkins (1896) declared that plethodontids have a partial atrial septum and that the S-A has shifted to the LA from the RA, where it is located in all other amphibians. Subsequent authors disagree regarding the position of the S-A and the degree of septation (Bruner, 1900; Noble, 1925; Putnam & Kelly, 1978; Fig. 1). The lack of agreement could be due to the different species that the authors examined or the different analytic techniques employed. Alternatively, it may be due to the failure of all studies but one (Putnam and Kelly, 1978) to directly compare plethodontids to lunged outgroups. Putnam & Kelly (1978) described the atrial septum of lunged salamanders as a complex of two components, IA and IB, which appear equivalent to our components AS1 and AS2, respectively.

Hopkins (1896) asserted that the S-A lies within the left atrium, but he failed to recognize the two-part nature of the atrial septum, which is apparent when one compares plethodontids to lunged outgroups (Figs 1 and 7). The S-A is left of AS1, but in lunged salamanders the RA extends dorsal to the LA and the loss of AS2 makes it appear that the S-A is in the LA. Putnam and Kelly (1978) were largely correct in their interpretation of atrial morphology and the position of the S-A, but they failed to recognize the artifactual nature of Hopkins' account, which led them to incorrectly depict the position of the S-A relative to AS1 in their figures. Bruner (1900) did observe tissue within the atrium, but he interpreted this tissue as the sinoatrial valve. Cords (1923) supported Bruner's view. Our data suggest that the sinoatrial valve in both plethodontids and lunged salamanders is formed by a distinct flap of tissue at the dorsal base of AS1 (Figs S4 and 2C,D), and this interpretation is supported in the literature (Putnam & Kelly, 1978; Putnam & Parkerson, 1985). It is unlikely, as Bruner (1900) and Cords (1923) assert, that the entirety of AS1 functions as a sinoatrial valve, although AS1 may play a functional role as a point of attachment for the sinoatrial valve. It is also possible that AS1 plays a developmental role in the formation of other cardiac structures such as the sinoatrial and atrioventricular valves. Alternatively, AS1 may play no physiological role and is retained as a vestige due to low selective pressure for its loss. Elasmobranchs, which lack lungs and atrial septa, possess paired sinoatrial valves flanking the S-A but not a unilateral flap valve (Hamlett *et al.* 1996; Ramos *et al.* 1996). The elasmobranch condition may support the hypothesis that a structure traversing the atrium, such as AS1, is not necessary for the sinoatrial valve to function.

Several early authors declared that salamanders have a highly fenestrated atrial septum (reviewed in Noble, 1925). However, Noble (1925) did not observe this condition in salamanders with mostly pulmonary respiration. He suggested instead that fenestration is a feature of species that predominately use non-pulmonary respiration, such as *Rhyacotriton olympicus* and *Cryptobranchus alleganiensis* (Noble, 1925; Putnam & Parkerson, 1985). Interestingly, *R. olympicus*, which possesses vestigial lungs, retains a fully developed but fenestrated AS. A number of caecilians with reduced reliance on pulmonary respiration also show partial reduction or fenestration of the atrial septum (Wilkinson & Nussbaum, 1997; de Bakker *et al.* 2015). We did not observe AS fenestration in lunged or lungless specimens. AS reduction and AS fenestration likely function similarly by accounting for reduced or absent pulmonary return with appropriate shunting of blood between atria (Lawson, 1966).

### Convergent reduction of the atrial septum

Our data support at least two independent evolutionary losses of AS2 in salamanders, one in the lungless family Plethodontidae and a second in the completely lungless genus *Onychodactylus* (Hynobiidae). *Salamandrina perspicillata*, a salamandrid species with reduced lungs, also may have lost AS2, as illustrated in one published drawing: Cords (1923) depicts a septum covering the S-A when viewed anteriorly. This septum is likely the AS1, which has been reflected posteriorly. If our interpretation is correct, then the AS2 has been lost independently at least three times in salamanders, further underscoring the functional importance of septum reduction during the evolution of lunglessness and/or the existence of a shared developmental mechanism that links lung loss/reduction and septal reduction.

Cords (1923) closes her manuscript by noting the crucial importance of further research on the atrial septum in salamanders. She asks whether the AS develops fully and subsequently regresses in lungless or lung-reduced salamanders, or if instead it fails to develop fully. Our data, drawn from

**Fig. 4.** Micro-CT sections through an adult heart of *Plethodon cinereus*. (A) Frontal sections at 57-μm increments from ventral to dorsal illustrate the components of the heart. Sections are arranged from left to right, top to bottom. (B) Volume renderings of the heart from a ventral perspective. Cutaway (right) reveals AS1, segmented in purple. AS1, atrial septum component 1; A-V, atrioventricular aperture; LA, left atrium; OFT, outflow tract; RA, right atrium; S-A, sinoatrial aperture; SV, sinus venosus; V, ventricle.

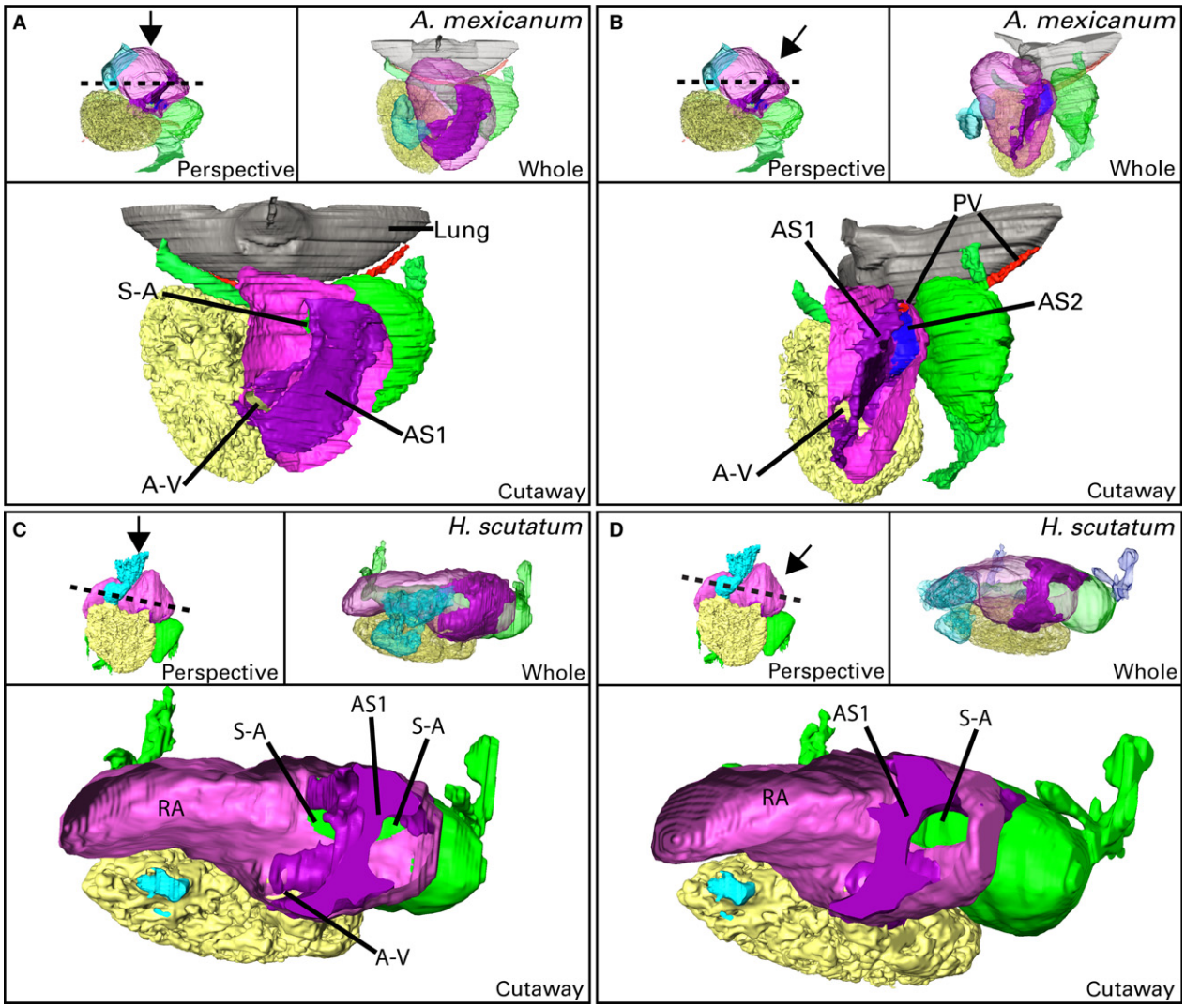


**Fig. 5.** Comparative morphology of the posterior atrial wall. (A–D) Each pair of insets depicts the angle of cutaway and viewing, as well as a whole transparent heart viewed from the same angle as the cutaway. (A) Cutaway into the atria of a stage-57 *Ambystoma mexicanum* (lunged) heart from an anterior perspective. The S-A is visible. (B) The heart in (A) viewed from a left lateral angle reveals AS2 and the pulmonary vein inlet. The S-A is not visible because it is covered by AS2. (C) Cutaway into the atria of a 16.5 mm (total length) larva *Hemidactylium scutatum* (lungless) heart depicted from an anterior perspective. The S-A is visible on both sides of AS1. (D) Left lateral view of the heart in (C) reveals the lack of AS2 and, consequently, the ability to see the S-A through the presumptive LA. AS1, atrial septum component 1; AS2, atrial septum component 2; A-V, atrioventricular aperture; PV, pulmonary vein; RA, right atrium; S-A, sinoatrial aperture; V, ventricle.

multiple ontogenetic stages of plethodontid salamanders, supports the latter proposition.

### Atrial septum development

The AS complex is slow to develop in *A. mexicanum*, a lunged species. At hatching, AS2 is present but AS1 is small. During larval stages, AS1 grows to fully partition the atrium (Figs S1 and S2). In lungless plethodontids, AS1 is present at hatching but shows no sign of further development during larval or juvenile stages. In the frog *Xenopus laevis*, the atrial septum is one of the last heart structures to develop (Mohun *et al.* 2000). The atrial septum originates from the dorsal wall of the atrium; the AS then extends towards the atrioventricular opening, eventually separating the two atria (Simons, 1957; Mohun *et al.* 2000; de Bakker *et al.* 2015). Our results on AS growth are consistent with these findings (Figs S1 and S2), but we did not examine the earliest stages of *A. mexicanum* to determine the precise origin of the AS.

The mammalian atrial septum is a composite of tissues from multiple embryonic origins (Briggs et al. 2012). The septum begins to develop from the dorsal portion of the common atrium with the formation of the myocardium-derived septum primum, which is covered in an endocardium-derived mesenchymal cap. The septum primum

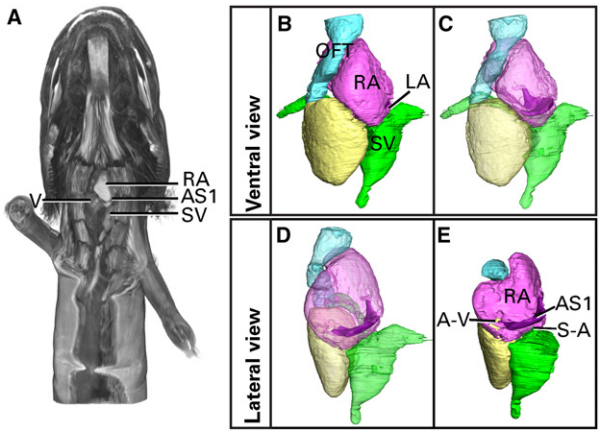


**Fig. 6.** Atrial morphology in the convergently lungless species *Onychodactylus japonicus*. (A) Frontal orthoslice through a contrast-stained μ-CT scan at the level of the heart. Atrial chambers are radiopaque due to the dense mass of blood contained within them. The AS1 is visible as a less-opaque structure positioned far towards the left edge of the atrium. Ventral view of the segmented heart rendered opaque (B) and transparent (C) to view the atrial chambers and the AS1. Lateral views of the *O. japonicus* heart rendered transparent (D) and opaque with a cutaway (E). Cutaway view reveals the S-A and A-V. AS1, atrial septum component 1; A-V, atrioventricular aperture; LA, left atrium; OFT, outflow tract; RA, right atrium; S-A, sinoatrial aperture; SV, sinus venosus; V, ventricle.

elongates into the common atrium alongside the DMP, which is a mesenchymal tissue derived from extracardiac second-heart-field mesoderm that enters the heart through the dorsal mesocardium. The atrial septum forms from the coalescence of the DMP/septum primum extension and the atrioventricular cushions (Briggs et al. 2012; Wessels, 2016). The pulmonary vein, which forms from a midline diverticulum from the heart into the dorsal mesocardium, is displaced into the left atrium by the evagination of the DMP into the common atrium (Briggs et al. 2012).

Recent developmental-genetic studies highlight the importance of signaling interactions and genetic pleiotropy between the lungs and heart during organogenesis. From the characterization of human birth defects, there is increasing awareness that many critical heart development genes play pleiotropic roles in the development of other organs (reviewed in Li *et al.* 1997). For instance, Holt-Oram syndrome, which is due to a mutation in the T-box transcription factor Tbx5, is characterized by atrial septal defects, upper limb malformation and occasional right lung agenesis (Basson *et al.* 1997; Li *et al.* 1997; Tseng *et al.* 2007). Tbx5 is known to regulate Fgf10 expression in the developing limb (Agarwal *et al.* 2003) and is important for lung branching (Cebra-Thomas *et al.* 2003). Congenital ASDs also include cor triloculare biventriculare, or complete absence of the atrial septum (Sangam *et al.* 2011), which, based on associated malformations that include polydactyly and cleft palate, is likely due to a defect in the Shh pathway (personal observation, Zachary R. Lewis (ZRL)). Ellis-Van Creveld syndrome, which is caused by a mutation in a positive mediator of Shh signaling, results in ASDs (Baujat & Le Merrer, 2007). Mouse mutants for the important pulmonary gene Wnt2 also lack atrial septa (Tian *et al.* 2010). Finally, crucial mediators of both lung and AS development include members of the Bmp pathway such as Alk3, Bmp4 and Osr1 (Jiao *et al.* 2003; Briggs *et al.* 2013; Zhou *et al.* 2015). Osr1 mutations result in ASDs and lung phenotypes (Wang *et al.* 2005; Xie *et al.* 2012), and knockdown of Osr1 and Osr2 results in lung loss (Rankin *et al.* 2012). All these Bmp signaling-associated genes play essential roles in both heart and lung morphogenesis. Interestingly, several defects associated with mutations of these genes have orthologous phenotypes to those displayed in lungless salamander hearts (*viz.* left atrium hypoplasia, atrial septal defects and lack of pulmonary circulation). In a rare instance of human lung loss, an ASD is also present (Devi & More, 1966).

Research on heart septation in mice implicates pulmonary and pharyngeal endoderm in producing morphogens that are directly responsible for development of the atrial septum and the outflow tract, respectively (Goddeeris *et al.* 2007, 2008; Hoffmann *et al.* 2009, 2014). Shh secreted from the tracheal pulmonary endoderm to the second-heart-field mesoderm potentiates a population of cells that migrate into the heart and form the DMP. Subsequent work pinpoints activation of Foxf genes by Gli1 and Tbx5 as critical for pulmonary-induced septal morphogenesis (Hoffmann *et al.* 2014). The above results imply a direct molecular link between lung and heart morphogenesis during the evolution of cardio-pulmonary respiration.

Provided that the mechanism of atrial septum development is conserved between amphibians and mammals, there may be a direct causal link between lung loss and atrial septum reduction. It is possible that the absence of lungs is associated with decreased Shh signaling to the second-heart-field mesoderm during lungless salamander embryonic development. This, in turn, may result in hypoplasia of the DMP and atrial septum reduction. In particular, it is possible that AS2 in lunged salamanders is derived from the DMP, whereas AS1 is derived from the septum primum. If true, then lungless salamanders may be missing AS2 due to the failure of cells from the second heart field to migrate into the heart. It may be possible to test these predictions by examining the embryological origins of AS1 and AS2 in lunged and lungless salamanders, which we hypothesize to be myocardial and extracardiac, respectively. As the partial atrial septum of adult *P. cinereus* is composed of both myocardial and endocardial tissue (Fig. S4), it is difficult to determine the embryonic origin of each tissue type retroactively because the septum primum is composed of both myocardial and endocardial tissue, while the DMP is composed of endocardial-like mesenchymal tissue that later undergoes mesenchymal to myocardial differentiation.

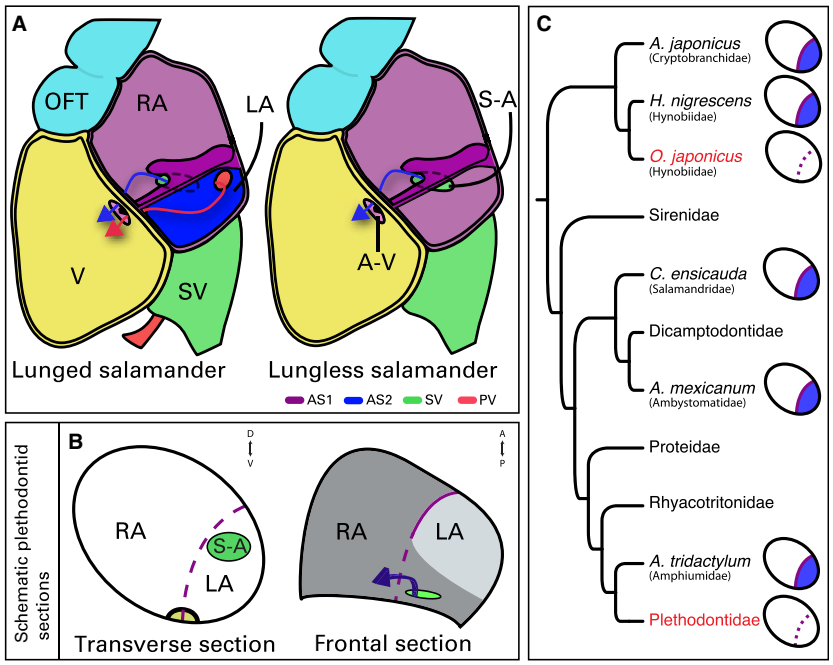


**Fig. 7.** Atrial morphology in salamanders. (A) Lunged salamanders have two sources of blood to the atrium: the SV (via S-A) and the pulmonary vein. Blood from S-A passes dorsal to AS2 and then posterodorsal through the emarginated portion of AS1, and then through A-V (blue arrow). Blood from the pulmonary vein passes ventral to AS2 before flowing through A-V (red arrow). Lungless salamanders lack pulmonary veins and AS2, so blood from SV could presumably flow freely between atrial chambers. (B) Schematic sections of plethodontid atria. When viewed from the anterior, the S-A appears displaced to the left side of AS1, a condition that some previous authors took to indicate that S-A had shifted to the left atrium. When AS1 is interpreted as just a component of the bipartite atrial septal complex, it is clear that the RA (shaded region in frontal section) extends posterodorsal to the left atrium. The lack of AS2 accounts for the assignment of this region to the LA. Comparison to lunged outgroups (e.g. Fig. 2F) is necessary for making this assessment. (C) Convergent evolutionary reduction of atrial septa occurs in different lineages of lungless salamanders. A cladogram shows the evolutionary relationships among extant salamanders (Pyron & Wiens, 2011), along with their atrial morphology in schematic transverse view. Lungless groups are indicated in red. The species examined in the present study are indicated with their Latin name, except in the case of the species in Plethodontidae, which are listed in Table 1. *Ambystoma mexicanum, Amphiuma tridactylum, Andrias japonicus, Cynops ensicauda, Hynobius nigrescens, Onychodactylus japonicus*. Families are listed in roman type. AS1, atrial septum component 1; A-V, atrioventricular aperture; LA, left atrium; OFT, outflow tract; RA, right atrium; S-A, sinoatrial aperture; SV, sinus venosus; V, ventricle.

## Conclusion

Convergent evolution is a fascinating yet vexing phenomenon in systematic and morphological research. There are several developmental mechanisms by which convergent morphologies might arise (Manceau *et al.* 2010; Stern, 2013). These include independent mutations of a single gene, mutations of multiple genes within a pathway, selection on standing genetic variation, and introgression of loci (Stern, 2013). Certain convergent traits may also emerge as pleiotropic effects of selection on molecularly or developmentally linked phenotypes. The heart and lungs function as an integrated system; functional mismatch between them would have disastrous consequences for organismal physiology. We propose that the molecular crosstalk between the developing lungs and heart may underlie convergent reduction of the atrial septum across species of lungless salamanders. Our study supports a process by which pleiotropic interactions between developing heart and lung pattern the co-evolution of the functionally constrained cardiopulmonary system.

## Acknowledgements

We acknowledge the following assistance: H. Maddin – μ-CT scanning and reconstruction; J. Rosado – access to MCZ specimens; B. Cooke, C. Eng, J. Dorantes, J. Martinez, S. Tilley, M. Hawkins, N. Piekarski, M. McCarroll, Y. Wu, J. Wu, D. Woolf, A. Koomas, A. Saunders, H. Maddin, E. Sefton, A. Sahay, M. Laslo and M. Aja – field collection; Caroline DeVane and Anne Everly – animal husbandry. Funding sources (Z.R.L.): NSF Graduate Research Fellowship; Kenneth Miyata Grant, Museum of Comparative Zoology; and a Robert G. Goelet Summer Research Award, Museum of Comparative Zoology.

## References

**Agarwal P, Wylie JN, Galceran J, et al.** (2003) Tbx5 is essential for forelimb bud initiation following patterning of the limb field in the mouse embryo. *Development* **130**, 623–633.

**de Bakker DM, Wilkinson M, Jensen B** (2015) Extreme variation in the atrial septation of caecilians (Amphibia: Gymnophiona). *J Anat* **226**, 1–12.

**Barrows AI** (1900) Respiration of *Desmognathus*. *Anat Anz* **18**, 461–464.

**Basson CT, Bachinsky DR, Lin RC, et al.** (1997) Mutations in human cause limb and cardiac malformation in Holt-Oram syndrome. *Nat Genet* **15**, 30–35.

**Baujat G, Le Merrer M** (2007) Ellis-Van Creveld syndrome. *Orphanet J Rare Dis* **2**, 27.

**Bickford D, Iskandar D, Barlian A** (2008) A lungless frog discovered on Borneo. *Curr Biol* **18**, 374–375.

**Bjornard K, Riehle-Colarusso T, Gilboa SM, et al.** (2013) Patterns in the prevalence of congenital heart defects, metropolitan Atlanta, 1978 to 2005. *Birth Defects Res Part A Clin Mol Teratol* **97**, 87–94.

**Bordzilovskaya N, Dettlaff T, Duhon S, et al.** (1989) Developmental-stage series of axolotl embryos. In: *Developmental Biology of the Axolotl* (eds Armstrong J, Malacinski G), pp. 201–219. Oxford: Oxford University Press.

**Briggs LE, Phelps AL, Brown E, et al.** (2013) Expression of the BMP receptor Alk3 in the second heart field is essential for development of the dorsal mesenchymal protrusion and atrioventricular septation. *Circ Res* **112**, 1420–1432.

**Briggs LE, Kakarla J, Wessels A** (2012) The pathogenesis of atrial and atrioventricular septal defects with special emphasis on the role of the dorsal mesenchymal protrusion. *Differentiation* **84**, 117–130.

**Bruner HL** (1900) On the heart of lungless salamanders. *J Morphol* **16**, 323–336.

**Cebra-Thomas JA, Bromer J, Gardner R, et al.** (2003) T-box gene products are required for mesenchymal induction of epithelial branching in the embryonic mouse lung. *Dev Dyn* **226**, 82–90.

**Cords E** (1923) Das Herz eines lungenlosen Salamanders (*Salamandrina perspicillata*). *Anat Anz* **57**, 205–213.

**Davies F, Francis ETB** (1941) The heart of the salamander (*Salamandra salamandra*, L.), with special reference to the conducting (connecting) system and its bearing on the phylogeny of the conducting systems of mammalian and avian hearts. *Philos Trans R Soc B* **231**, 99–130.

**Devi B, More JRS** (1966) Total tracheopulmonary agenesis associated with asplenia, agenesis of umbilical artery and other anomalies. *Acta Paediatr Scand* **55**, 107–116.

**El-Said G, Mullins CE, Mcnamara, DG** (1972) Management of total anomalous pulmonary venous return. *Circulation* **45**, 1240–1250.

**Goddeeris MM, Schwartz R, Klingensmith J, et al.** (2007) Independent requirements for hedgehog signaling by both the anterior heart field and neural crest cells for outflow tract development. *Development* **134**, 1593–1604.

**Goddeeris MM, Rho S, Petiet A, et al.** (2008) Intracardiac septation requires hedgehog-dependent cellular contributions from outside the heart. *Development* **135**, 1887–1895.

**Gould SJ** (1980) The evolutionary biology of constraint. *Daedalus* **109**, 39–52.

**de Graaf AR** (1957) Investigations into the distribution of blood in the heart and aortic arches of *Xenopus laevis* (Daud.). *J Exp Biol* **34**, 143–172.

**Haberich F** (1965) The functional separation of venous and arterial blood in the univentricular frog heart. *Ann N Y Acad Sci* **127**, 459–476.

**Hamlett WC, Schwartz FJ, Schmeinda R, et al.** (1996) Anatomy, histology, and development of the cardiac valvular system in elasmobranchs. *J Exp Zool* **275**, 83–94.

**Hoffmann AD, Peterson MA, Friedland-Little, JM, et al.** (2009) Sonic hedgehog is required in pulmonary endoderm for atrial septation. *Development* **136**, 1761–1770.

**Hoffmann, AD, Yang XH, Burnicka-Turek O, et al.** (2014) Foxf genes integrate Tbx5 and Hedgehog pathways in the second heart field for cardiac septation. *PLoS Genet* **10**, e1004604.

**Hopkins G** (1896) The heart of some lungless salamanders. *Am Nat* **30**, 829–833.

**Hurney CA, Babcock SK, Shook DR, et al.** (2015) Normal table of embryonic development in the four-toed salamander, *Hemidactylium scutatum*. *Mech Dev* **136**, 99–110.

**Jensen B, Moorman AFM** (2016) Evolutionary aspects of cardiac development. In: *Congenital Heart Diseases: The Broken Heart: Clinical Features, Human Genetics and Molecular Pathways*. (eds Rickert-Sperling S, Kelly RG, Driscoll DJ.), pp. 109–117. Vienna: Spring-Verlag.

**Jensen B, Wang T, Christoffels VM, et al.** (2013) Evolution and development of the building plan of the vertebrate heart. *Biochim Biophys Acta* **1833**, 783–794.

**Jiao K, Kulessa H, Tompkins K, et al.** (2003) An essential role of Bmp4 in the atrioventricular septation of the mouse heart. *Genes Dev* **17**, 2362–2367.

**Johansen K** (1962) Double circulation in the amphibian *Amphiuma tridactylum*. *Nature* **194**, 991–992.

**Johansen K** (1963) Cardiovascular dynamics in *Amphiuma tridactylum*, PhD Diss. University of Oslo.

**Johansen K, Hanson D** (1968) Functional anatomy of the hearts of lungfishes and amphibians. *Am Zool* **8**, 191–210.

**Kerney R** (2011) Embryonic staging table for a direct-developing salamander, *Plethodon cinereus* (Plethodontidae). *Anat Rec* **294**, 1796–1808.

**Koshiba-Takeuchi K, Mori AD, Kaynak BL, et al.** (2009) Reptilian heart development and the molecular basis of cardiac chamber evolution. *Nature* **461**, 95–98.

**Lawson R** (1966) The anatomy of the heart of *Hypogeophis rostratus* (Amphibia, Apoda) and its possible mode of action. *J Zool* **149**, 320–336.

**Li QY, Newbury-Ecob RA, Terrett JA, et al.** (1997) Holt-Oram syndrome is caused by mutations in TBX5, a member of the brachyury (T) gene family. *Nat Genet* **15**, 21–29.

**Manceau M, Domingues VS, Linnen CR, et al.** (2010) Convergence in pigmentation at multiple levels: mutations, genes and function. *Philos Trans R Soc B* **365**, 2439–2450.

**Metscher BD** (2011) X-Ray microtomographic imaging of intact vertebrate embryos. *Cold Spring Harbor Protoc* **2011**, 1462–1471.

**McMullen EC** (1938) The morphology of the aortic arches in four genera of plethodontid salamanders. *J Morphol* **62**, 559–597.

**Mohun TJ, Leong LM, Weninger WJ, et al.** (2000) The morphology of heart development in *Xenopus laevis*. *Dev Biol* **218**, 74–88.

**Noble GK** (1925) The integumentary, pulmonary, and cardiac modifications correlated with increased cutaneous respiration in the Amphibia: a solution of the 'hairy frog' problem. *J Morphol* **40**, 341–416.

**Nussbaum RA, Wilkinson M** (1995) A new genus of lungless tetrapod: a radically divergent caecilian (Amphibia: Gymnophiona). *Proc R Soc Lond Ser B Biol Sci* **261**, 331–335.

**Nye HLD, Cameron JA, Chernoff EAG, et al.** (2003) Extending the table of stages of normal development of the axolotl: limb development. *Dev Dyn* **226**, 555–560.

**Parker SE, Mai CT, Canfield MA, et al.** (2010) Updated National Birth Prevalence estimates for selected birth defects in the United States, 2004–2006. *Birth Defects Res Part A Clin Mol Teratol* **88**, 1008–1016.

**Presnell JK, Schreibman MP, Humason GL** (1997) *Humason's Animal Tissue Techniques*, 5th edn. Baltimore: Johns Hopkins University Press.

**Putnam J, Kelly D** (1978) A new interpretation of interatrial septation in the lungless salamander, *Plethodon glutinosus*. *Copeia* **1978**, 251–254.

**Putnam J, Parkerson Jr. J** (1985) Anatomy of the heart of the Amphibia II. *Cryptobranchus alleganiensis*. *Herpetologica* **41**, 287–298.

**Pyron RA, Wiens JJ** (2011) A large-scale phylogeny of Amphibia including over 2800 species, and a revised classification of extant frogs, salamanders, and caecilians. *Mol Phylogenet Evol* **61**, 543–583.

**Ramos C, Muñoz-Chápuli R, Navarro P** (1996) Ultrastructural study of the myocardium of the sinus venosus and sinoatrial valve in the dogfish (*Scyliorhinus canicula*). *J Zool Lond* **238**, 611–621.

**Rankin SA, Gallas AL, Neto A, et al.** (2012) Suppression of Bmp4 signaling by the zinc-finger repressors Osr1 and Osr2 is required for Wnt/β-catenin-mediated lung specification in *Xenopus*. *Development* **139**, 3010–3020.

**Sangam MR, Devi SSS, Krupadanam K, et al.** (2011) Cor triloculare biventriculare with left superior vena cava. *Folia Morphol (Warsz)* **70**, 135–138.

**Seelye A** (1906) Circulatory and respiratory systems of *Desmognathus fusca*. *Proc Boston Soc Nat Hist* **32**, 335–357.

**Simons J** (1957) The pulmonary return as an agent in the final development of the atrium in *Rana temporaria*. *J Embryol Exp Morphol* **5**, 250–255.

**Stern DL** (2013) The genetic causes of convergent evolution. *Nat Rev Genet* **14**, 751–764.

**Taussig H** (1960) *Congenital Malformations of the Heart*. Cambridge: Harvard University Press.

**Tian Y, Yuan L, Goss AM, et al.** (2010) Characterization and *in vivo* pharmacological rescue of a Wnt2-Gata6 pathway required for cardiac inflow tract development. *Dev Cell* **18**, 275–287.

**Tseng YR, Su YN, Lu FL, et al.** (2007) Holt–Oram syndrome with right lung agenesis caused by a *de novo* mutation in the TBX5 gene. *Am J Med Genet Part A* **143**, 1012–1014.

**Wang Q, Lan Y, Cho E-S, et al.** (2005) Odd-skipped related 1 (Odd 1) is an essential regulator of heart and urogenital development. *Dev Biol* **288**, 582–594.

**Wessels A** (2016) Inflow tract development. In: *Congenital Heart Diseases: The Broken Heart: Clinical Features, Human Genetics and Molecular Pathways*. (eds Rickert-Sperling S, Kelly, RG, Driscoll DJ), pp. 55–62. Vienna: Spring-Verlag.

**Whitford WG, Hutchison VH** (1965) Gas exchange in salamanders. *Physiol Zool* **38**, 228–242.

**Wilder HH** (1896) Lungless salamanders. *Anat Anz* **12**, 182–192.

**Wilkinson M, Nussbaum RA** (1997) Comparative morphology and evolution of the lungless caecilian *Atretochoana eiselti* (Taylor) (Amphibia: Gymnophiona: Typhlonectidae). *Biol J Linn Soc* **62**, 39–109.

**Xie L, Hoffmann AD, Burnicka-Turek O, et al.** (2012) Tbx5-hedgehog molecular networks are essential in the second heart field for atrial septation. *Dev Cell* **23**, 280–291.

**Yoshikawa N, Matsui M** (2014) A new salamander of the genus *Onychodactylus* from Tsukuba Mountains, eastern Honshu, Japan (Amphibia, Caudata, Hynobiidae). *Zootaxa* **3866**, 53–78.

**Yoshikawa N, Matsui M, Nishikawa K, et al.** (2008) Phylogenetic relationships and biogeography of the Japanese clawed salamander, *Onychodactylus japonicus* (Amphibia: Caudata: Hynobiidae), and its congener inferred from the mitochondrial cytochrome b gene. *Mol Phylogenet Evol* **49**, 249–259.

**Zhou L, Liu J, Olson P, et al.** (2015) Tbx5 and Osr1 interact to regulate posterior second heart field cell cycle progression for cardiac septation. *J Mol Cell Cardiol* **85**, 1–12.

## Supporting Information

Additional Supporting Information may be found in the online version of this article:

**Fig. S1.** Histological sections through the heart of the lunged salamander *Ambystoma mexicanum* at stage 52.

**Fig. S2.** Histological sections through the heart of the lunged salamander *Ambystoma mexicanum* at stage 57.

**Fig. S3.** The atrial septum of the swordtail newt, *Cynops ensicauda*

**Fig. S4.** Reconstruction of the atrial septum in adult *Plethodon cinereus* based on histological sections.

**Table S1.** Collection localities for plethodontid salamanders. All localities are in Massachusetts, USA.

**Video S1.** 3-D histological reconstruction of the heart of the lunged salamander *Ambystoma mexicanum* at stage 52.

**Video S2.** 3-D histological reconstruction of the heart of the lunged salamander *Ambystoma mexicanum* at stage 57.

**Video S3.** 3-D volume rendering of the heart of an adult lungless salamander (*Plethodon cinereus*).